Groundwater for Sustainable Development 15 (2021) 100650

Contents lists available at ScienceDirect

Groundwater for Sustainable Development

journal homepage: www.elsevier.com/locate/gsd

Research paper

Hydrochemistry and fluoride contamination in Ndali-Kasenda crater lakes, Albertine Graben: Assessment based on multivariate statistical approach and human health risk

Walter Ojok [a,b,*], William Wanasolo [d], John Wasswa [c], James Bolender [e], Emmanuel Ntambi [a]

[a] Department of Chemistry, Faculty of Science, Mbarara University of Science and Technology, P.O Box 1410, Mbarara, Uganda
[b] Department of Chemistry, Faculty of Science, Muni University, P.O Box 725, Arua, Uganda
[c] Department of Chemistry, College of Natural Sciences, Makerere University, P.O Box 7062, Kampala, Uganda
[d] Department of Chemistry, Faculty of Science, Kyambogo University, P.O Box 1, Kyambogo, Kampala, Uganda
[e] Department of Chemistry and Biochemistry, University of San Diego, 5998 Alcalà Park, San Diego, CA, 92110, USA

ARTICLE INFO

Keywords:
Fluoride
Ndali-kasenda
Albertine graben
Hydrochemistry
Multivariate statistics
Crater lakes

ABSTRACT

Hydrochemistry of crater lakes (n = 15) in the Ndali-Kasenda cluster was deciphered using standard methods of the American Public Health Association to understand the major ion chemistry; spatial distribution, occurrence, and non-carcinogenic health risks due to exposure to fluoride levels in the lakes in Ndali- Kasenda cluster, Albertine Graben. Numerous economic activities take place in and around the crater lakes which serve as major sources of domestic water whose origin of potential contaminants is ambiguous. In this study, WHO (2017) regulatory limit exceedance included F^-, pH, Ca^{2+}, Fe^{2+}, Mn^{2+}, and TDS. A strong positive correlation was observed between F^- and TDS; F^- and pH; F^- and EC; F^- and HCO_3^-. However, concerning hydrogeochemical signature, the lakes are mainly of Ca–HCO_3 type and low in Na–K–HCO_3 type due to rock water interaction in the geology of the area. Principal component analysis (PCA) performed on Ndali-Kasenda hydrogeochemical data resulted in six principal components (PCs) explaining 88.6% of the total variance. The PCs represented the primary processes that control the crater lake hydrogeochemistry in the Ndali-Kasenda area which include; weathering of rocks reactions, ion exchange, and evaporation processes. The hazard quotient (HQ) for non-carcinogenic health risks associated with exposure to Ndali- Kasenda fluoride levels via ingestion revealed that HQ for infants surpassed the acceptable HQ limit for all the lakes studied, while 86.67 % of the sampled lakes exceeded the HQ value for children via ingestion. Based on the hydrogeochemical parameters analyzed, aside from L. Murigamire and L. Wankenzi, water from the other studied lakes is chemically not acceptable for drinking purposes. An urgent need to take ameliorative action in this area to protect the inhabitants from exposure to excess fluoride in drinking water was recommended.

1. Introduction

Volcanic crater lakes are unique important natural resources with the capacity to provide drinking water and several other ecosystem services to humans (Nankabirwa et al., 2019; Rubaihayo et al., 2008). However, this ability is threatened by the occurrence of elevated levels of mineral ions of geogenic and anthropogenic origins (Nankabirwa et al., 2019; Tumwebaze et al., 2019). For instance, over 37% of the inhabitants in the Ndali-Kasenda area obtain their water for domestic use from crater lakes (Rubaihayo et al., 2008) whose origin of potential contaminants is ambiguous. Fluorine is the 13th most abundant mineral in the earth crust and occurs in water resources in varying proportions depending on the plethora of fluoride-bearing minerals in the underlying rocks (Ali et al., 2018, 2019; Kashyap et al., 2020; Thakur et al., 2013). Fluoride in water sources emanates from anthropogenic and geogenic sources (Ali et al., 2019; Dongzagla et al., 2019; Kashyap et al., 2020; Ali et al., 2016; Thakur et al., 2013; Tiwari et al., 2020). The application of pesticides and fertilizers containing organic fluorine is the predominant anthropogenic source of fluoride in surface waters. However, groundwater in the study area is predominantly impacted by geogenic sources of soluble fluoride-containing minerals (Ijumulana et al., 2020; Kimambo et al., 2019; Smedley et al., 2002). More than 150 fluoride-rich minerals occur

* Corresponding author. Department of Chemistry, Faculty of Science, Mbarara University of Science and Technology, P.O Box 1410, Mbarara, Uganda.
E-mail address: w.ojok@muni.ac.ug (W. Ojok).

https://doi.org/10.1016/j.gsd.2021.100650
Received 18 January 2021; Received in revised form 16 July 2021; Accepted 30 July 2021
Available online 8 August 2021

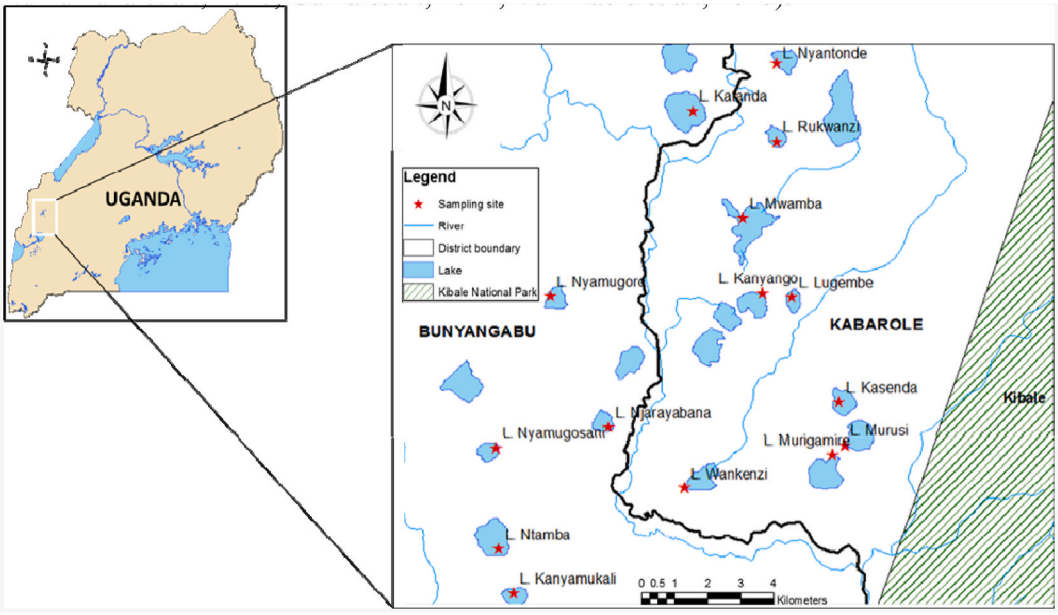

Fig. 1. Location of sampled crater lakes in the Ndali-Kasenda cluster.

in the upper layers of the earth's lithosphere, with the most abundant sources being clay and silicate minerals (Chandrajith et al., 2020; Kimambo et al., 2019; Thakur et al., 2013; Tiwari et al., 2020). In arid and semi-arid regions of the world, high rates of evaporation and low precipitation exacerbate fluoride enrichment (Chandrajith et al., 2020; Tiwari et al., 2020) in groundwater-fed surface water sources. Thus, the occurrence of fluoride at elevated levels in water for drinking is a serious problem in arid and semiarid regions of the world, affecting an estimated 200 million people worldwide (Kashyap et al., 2020; Tiwari et al., 2020; Wanke et al., 2017). Nevertheless, humans are mainly exposed to fluoride contamination by ingestion of water with elevated fluoride levels (Ali et al., 2018; Kimambo et al., 2019). Depending on its concentration, fluoride may have beneficial or harmful effects on human health. Exposure to low fluoride concentrations (0.5–1.5 mg/L) helps prevent tooth decay by inhibiting lactic acid production by bacteria on the tooth surface. However, ingestion of excess fluoride above 1.5 mg/L has detrimental health effects with varying mechanisms of toxicity. In the human gut, fluoride ions combine with protons from the gastrointestinal mucosa to form hydrofluoric acid, which is then absorbed leading to abdominal pains, diarrhea, nausea, gastrointestinal irritation, and vomiting (Ali et al., 2018; Edmunds and Smedley, 2005; Toolabi et al., 2021). Chronic ingestion of fluoride ladened water (1.5 mg/L - 4.0 mg/L) leads to the development of dental fluorosis, the permanent disruption of enamel production in children. Dental fluorosis is characterized by discolored, blackened, mottled, or chalky white/brown teeth (Edmunds and Smedley, 2005; Ijumulana et al., 2020; Toolabi et al., 2021). Ingestion of higher fluoride concentration (>4.0 mg/L) may result in skeletal fluorosis, which is a malformation of bone structure (Chandrajith et al., 2020; Onipe et al., 2020). Other reported health effects of excess fluoride ingestion include the retardation of physical and intellectual development in children, spontaneous abortion, neurological damage, kidney failure, and other forms of morbidities (Ali et al., 2019; Toolabi et al., 2021). At present, an estimated 80 million people are suffering from dental fluorosis and other fluoride-related morbidities in East Africa (Ijumulana et al., 2020; Kimambo et al., 2019). Due to the health hazards of excess fluoride in drinking water, delineation of its release mechanism and its genesis in various water resources has received considerable attention from researchers in recent years (Ali et al., 2016; Kashyap et al., 2020; Kimambo et al., 2019). On that note, many researchers have studied sullying of water sources with fluoride (Egor and Birungi, 2020; Emenike et al., 2018; Ijumulana et al., 2020; Kashyap et al., 2020; Kimambo et al., 2019; Thakur et al., 2013; Tiwari et al., 2020). For example, Singh et al. (2013) used GIS and geochemical model WATEQ4F to map fluoride contamination in Allahabad District in India. Similarly, geochemical modeling of fluoride contamination was done to decipher the fluoride release mechanism in the hard rocks of Madhya Pradesh in India by Thakur et al. (2013). Their study employed saturation indices computation and found spatial fluoride variation ranging from 0.6 mg/L – 4.74 mg/L.

More recently, Tiwari et al. (2020) evaluated fluoride contamination in groundwater in a semi-arid region of India with fluoride concentration in the range 0.48 mg/L – 3.64 mg/L while Egor and Birungi (2020) found fluoride in the range 0.2 mg/L- 3.0 mg/L in the Sukulu hills in Eastern Uganda with an upper limit calculated using a modified Galagan equation found to be 0.4 mg/L. Relatedly, studies involving multivariate statistics and non-carcinogenic human health risks assessment using the US EPA (2011) through ingestion and dermal contact pathways were employed in South Western Nigeria (Emenike et al., 2018), Tanzania (Ijumulana et al., 2020), Sri Lanka (Chandrajith et al., 2020), Bangladesh (Bodrud-Doza et al., 2020), Iran (Toolabi et al., 2021), India (Mohanta et al., 2020), and North China (Chen et al., 2017). Their results showed the greater vulnerability of infants and children to high fluoride levels in the studied water resources. Although some researchers have done work on the crater lakes, hydrochemical and fluoride contamination in them is still at a nascent stage in the literature. Such a multidisciplinary approach for understanding the occurrence, spatial distribution of fluoride, and its associated health risks have not yet been carried out in the Ndali- Kasenda crater lakes located in the Albertine Graben which provide water for domestic use for over 37 % of the inhabitants located in the area. This study reports for the first time a multidisciplinary approach employing hydrogeochemical, multivariate statistics, and Human Health Risk Assessment (HHRA) model to interpret information on spatial variation of fluoride and its associated non-carcinogenic health risks via ingestion. Hence the main objectives of this present study were to:

i) determine hydrochemical characteristics of Ndali-Kasenda crater lakes serving as domestic water sources
ii) apply GIS, correlation, and multivariate statistical techniques to map spatial fluoride distribution and evaluate sources responsible for high fluoride in the crater lakes of Ndali- Kasenda cluster

iii) assess non-carcinogenic health risks due to exposure to fluoride within the crater lake system, using the HHRA model via ingestion pathway.

This study is envisaged to provide hydrogeochemical information for the development of efficient and effective management strategies and remedial measures for the provision of safe drinking water in rural communities in the vicinity of the Ndali- Kasenda area.

2. Materials and methods

2.1. Study area

The study area is located in the Albertine Rift system of Western Uganda within the longitude 030.223635–030.323199 E and latitude 0.400566–0.51935N (Fig. 1). The Ndali-Kasenda crater cluster is bordered by Kibale Forest National Park on the Eastern side with moist semi-deciduous forest. On the non-protected areas, however, the natural vegetation has been intensively modified through land use with widespread deforestation leaving the catchments susceptible to erosion and nutrient loss (John et al., 2008; Tumwebaze et al., 2019). Activities carried out in the area include crop farming (coffee, tea, banana, beans, cassava, potatoes), animal rearing (cattle, sheep, goats, pigs), agro-forestry, small-scale fishing, bird watching, and other forms of tourism. Most of the sampled lakes do not have outlets/inlets and provide water for domestic, agricultural, and dewatering tenacities (Nankabirwa et al., 2019; Tumwebaze et al., 2019). The area experiences a warm humid tropical climate with average annual precipitation being 926.5 mm. There is a bimodal rainfall pattern with peaks occurring during March to May and then again from October–December. The mean monthly temperatures are high, varying between 15.3 °C in December to 31.1 °C in February (Saulnier-Talbot et al., 2018; UBOS, 2019). The area lies partly within the Archaean basement rocks of the gneissic granulite complex of the Karagwe - Ankolean belt and the proterozoic metamorphosed rocks of the Buganda- Toro belt (de Dieu Ndikumana et al., 2020; Eby et al., 2009) (de Dieu Ndikumana et al., 2020). The geology of the Ndali- Kasenda area is hosted by recent volcanic rocks and alluvial deposits comprising of magmatised gneissic granulite complex interlayered with parts of the Buganda-Toro belt containing micaceous schists, amphibolites, quartzites, and calcsilicates. Furthermore, the Karagwe -Ankolean belt contains kamafugites and carbonatites (Guma et al., 2021; Van Daele et al., 2020) partly arising from volcanogenic carbon dioxide from the crater lakes (Bailey et al., 2005). However, the lake's hydrogeochemistry is governed by the pyrites, kaolinite, calcite, felsic granites, and vermiculite minerals occurring in the area (de Dieu Ndikumana et al., 2020; Guma et al., 2021; Van Daele et al., 2020).

2.2. Water sampling

Water samples were collected from 15 crater lakes which serve as water sources from August 2018 to March 2020. A total of 60 water samples were collected in 1.5-Liter clean polyethylene bottles from each of the studied crater lakes and appropriately labeled with sample ID. Sampling, preservation, and transport of water were carried out following standard protocols (APHA, 2012). Each site was sampled in triplicate and mixed to obtain a homogeneous sample, once every two months. Before sampling, the bottles were cleaned with spectroscopic nitric acid and then rinsed three times with water at the sampling sites. The samples were subsequently stored in 1.5-Liter plastic bottles in iceboxes at 4 °C before analysis to minimize Physico-chemical changes. Water samples for major ions were collected into clean 1.5-Liter polyethylene bottles while those for trace metals were collected and filtered using 0.45 μm Millipore filters into sterilized 12 mL polyethylene bottles. Concentrated nitric acid (0.5 mL) was added to each bottle with a sample for metal element analysis to stabilize them.

2.3. Analysis of water samples

Hydrochemical parameters were determined following standard methods of the American Public Health Association (APHA, 2012) and Vogels methods (Mendham, 2006). Water temperature, pH, electrical conductivity, dissolved oxygen, and total dissolved solids were measured in-situ using the HANNA Multiparameter meter (HANNA, Model HI9829). Sodium and potassium were measured using a flame photometer (Jenway, Model PFP7). Chloride was determined using argentometric titration with standard silver nitrate solution. Total dissolved phosphate was determined by the ascorbic acid method using a UV–Vis spectrophotometer (Jenway, Model 6305). Total hardness was measured by titration with standard hydrochloric acid and standard EDTA solution. Calcium and magnesium were determined by titration with standard EDTA. Aluminum, iron, and manganese were determined using a flame atomic absorption spectrophotometer (PerkinElmer model 2380). The concentration of bicarbonate and carbonate were determined volumetrically using standard hydrochloric acid. Sulfate ion concentration was determined by titration with standard barium chloride solution while nitrate was determined by UV–vis spectrophotometer (Jenway, Model 6305). The BOD_5 was determined by quantifying the dissolved oxygen of the water samples before and after incubation for 5 day at 20 °C while COD was determined by titration with potassium manganate VII solution. Fluoride was determined by a calibrated ion-selective electrode (HACH, Model 51,928–88) using the EPA method 9124 (Nelson, 2003).

Quality assurance was achieved through following standard laboratory procedures and quality control techniques: standardized calibration curve, replication, use of analytical grade reagents, reagent blanks, calibration of instruments while the accuracy of all chemical analyses was verified by computing ion charge balance error (CBE) for each sample using:

$$\%\ CBE = \frac{\sum cations - \sum anions}{\sum cations + \sum anions} \times 100 \quad (1)$$

The CBE values computed for all the 60 crater lake water samples were within the acceptable limit of ±10% (Chen et al., 2017).

2.4. Statistical and correlation analyses

The results of the hydrochemical analysis were subjected to descriptive statistical analysis where mean, minimum, maximum, standard deviation, and quartiles were calculated for each parameter using Statistical Package for the Social Sciences (SPSS) version 20.0 while hydrogeochemical facies were executed using Origin 2020b [OriginLab] software. All the hydrogeochemical data were analyzed statistically to provide general characteristics of the crater lakes. To assess the suitability of the lake waters for drinking purposes, the data was compared with the World Health Organization, (WHO, 2017), and US EPA (2018) water quality guidelines for drinking water. Map of the study area and spatial fluoride distribution in the Ndali-Kasenda crater lake cluster was achieved using ArcMap version 10.4.

2.5. Theory/calculation

2.5.1. Saturation indices

Geochemical modeling was performed using PHREEQC to compute aqueous phase speciation and mineral saturation indices of reactive minerals in the crater lakes (Kashyap et al., 2020; Singh et al., 2012). The mineral reactivity can be predicted using the PHREEQC model without collection of samples of the solid phase in an aquifer for mineralogical analyses (Dongzagla et al., 2019; Khatri et al., 2020; Nyam et al., 2020). This is because as groundwater flows, it interacts with the solid phase minerals in the geological formation of the aquifer leading to dissolution whereas precipitation occurs to reverse the process. Moreover, the saturation indices (SI) modeled by PHREEQC takes

Table 1
Descriptive statistics for hydrogeochemical characteristics of 15 lakes from Ndali-Kasenda crater lakes cluster (N = 60).

								Quartiles			Standards	
	Mean	MDL	MPL	Std. Deviation	Min.	Max.	% SEMPL	Q1	Q2	Q3	WHO (2017)	USEPA (2018)
Temp	25.76	–	–	1.89	23	30	–	24	25.4	27.3	–	–
EC	551.15	–	–	274.26	265	1180	6.67	346.25	396	707	1000	500[a]
pH	9.37	7	6.5–8.5	0.38	8.61	9.96	–	9.17	9.39	9.69	6.5–8.5	6.5–8.5
TDS	277.92	500	1000	134.39	136	586	–	173	215	351	1000	500
SO_4^{2-}	10.61	200	400	9.68	1	47.24	–	5	9.33	11.69	250	500
F^-	2.69	0.6	1.5	1.08	0.53	4.12	86.67	1.98	2.84	3.66	1.5	2.0
Cl^-	2.05	250	600	1.75	0.17	10	–	1.4	1.8	2.28	250	250
CO_3^{2-}	272.84	–	–	152.65	0	758.4	–	184.3	273.6	361.5	–	–
HCO_3^-	582.64	–	–	277.09	146.4	1307.84	–	341.6	531.92	857.66	500	–
NO_3^-	2.12	–	45	0.98	0.81	5.73	–	1.59	2.01	2.4	10	10
PO_4^{3-}	0.65	0.1	0.3	0.56	0.08	2.5	93.33	0.26	0.43	1.09	0.3	–
Na^+	12.12	–	200	7.53	4.25	32.0	–	6.5	10.17	14.1	200	95
K^+	2.62	10	12	1.44	0.9	6.30	–	1.5	2.1	3.2	10	–
Ca^{2+}	153.92	75	200	200.92	36	1540	6.67	68	84	197.5	200	–
Mg^{2+}	45.33	30	200	23.89	13.44	119.5	–	26.46	41.44	52.2	200	–
Al^{3+}	0.3	0.03	1	0.2	0.01	1.00	–	0.19	0.26	0.38	–	0.05–0.2
Fe	7.47	–	0.3	5.06	0	21.82	100	5.61	7.35	10.08	0.3	0.3
Mn^{2+}	0.447	0.05	0.1	0.461	0.1	1.7	80	0.2	0.3	0.5	0.1	0.05
TH	268.22	100	500	100.48	136	448	–	180	237	387	500	600
BOD	41.78	–	6	40.37	8.00	141.0	100	13	26	55	10	10[a]
COD	104.12	–	–	94.53	2.00	288.00	–	38	62	126	–	–
DO	5.79	4	6	2.63	0.8	10.8	46.67	3	6.6	7.92	4–6	8[a]

Max = Maximum; Min = Minimum; MDL = maximum desirable limit; MPL = Maximum permissible limit; % SEMPL = percentage of samples that exceed the maximum permissible limit; Q1 = 25th quartile; Q2 = 50th quartile; Q3 = 75th quartile; N = number of samples [a] = US EPA (2012). All data are in milligrams per liter (mg/L) except pH (no units), electrical conductivity (EC) in (μs/cm) and Temp = temperature in. °C

into account the interaction between groundwater and underlying rocks in the aquifer (Laxmankumar et al., 2019; Nyam et al., 2020; Singh et al., 2012).

The SI of a mineral is given by the equation

$$SI = logK_{IAP}/K_{sp} \quad (2)$$

where K_{IAP} is the ionic activity product while Ksp is the solubility product at a particular water temperature. Supersaturation of a given mineral is indicated by positive SI while negative SI signifies under saturation which favors the dissolution of minerals to attain equilibrium. Equilibrium condition in mineral saturation is indicated by SI of 0.5 (El Alfy et al., 2019; Nyam et al., 2020; Singh et al., 2012). Saturation indices of crater lakes' water obtained in this study were used to assess the mineral reactivity in the Ndali-Kasenda crater lake aquifer.

2.5.2. Fluoride exposure and health risk assessment

Health risk assessment is a corroborated method that has been used widely for evaluation of potential hazards of various chemicals on human health due to exposure over some time (Laxmankumar et al., 2019; Mohanta et al., 2020; Toolabi et al., 2021; US EPA, 1989, 2011). The United States Environmental Protection Agency (US EPA, 2011), identified several pathways through which humans can get exposed to chemical hazards such as inhalation, dermal, and ingestion pathways (US EPA, 2011).

To assess the health risks associated with fluoride within the Ndali-Kasenda crater lakes of Uganda, a human health risk assessment (HHRA) model was used to determine the non-carcinogenic adverse effects of exposure to elevated fluoride concentrations within the crater lake waters. The HHRA model has been widely adopted and used to develop mitigation strategies (Emenike et al., 2018; Ijumulana et al., 2020; Toolabi et al., 2021; US EPA, 1989, 2011) and applied in studies of human health risk in the United States of America (Bai et al., 2020), Tanzania (Ijumulana et al., 2020), South Western Nigeria (Emenike et al., 2018), Sri Lanka (Chandrajith et al., 2020), Bangladesh (Bodrud-Doza et al., 2020), Iran (Toolabi et al., 2021), India (Mohanta et al., 2020), and North China (Chen et al., 2017).

In this study, the non-carcinogenic health risks among the residents near the studied crater lakes due to ingestion of water from them were calculated from the daily fluoride intake and tolerable levels. As a result of variation in physiological and behavioral attributes in the population with age, the population was divided into the following groups: infants (0–2 years), children (3–11years), teenagers (12–19 years), and adults (20–65 years). The chronic daily dose of fluoride through ingestion was calculated using equation (3), based on US EPA, 1989) (Table S5) (Supplementary material).

$$EDI = \frac{C_f\ X\ IR\ X\ EF\ X\ ED}{BW\ X\ AT} \quad (3)$$

where:

EDI = estimated chronic daily dose of fluoride via ingestion (mg/kg. day).
C_f = concentration of fluoride in water.
IR = ingestion rate.
EF = resident exposure frequency (days/year).
ED = exposure duration (year).
BW = body weight (kg).
AT = averaging resident time (days/year).

Hazard quotient (HQ), an estimate of non-carcinogenic risks from exposure to fluoride through the pathway of ingestion was calculated using equation (4)

$$HQ = \frac{EDI}{RfD} \quad (4)$$

Where RfD is the reference dose of fluoride in a specific exposure pathway (mg/kg/day) obtained from the Integrated Risks Information System (IRIS) database of the US EPA. According to the IRIS database, the oral RfD for drinking water consumption is 0.06 mg/kg/day. When is HQ < 1; it implies a negligible risk of non-carcinogenic effects, whereas HQ > 1 indicates potential non-carcinogenic health effects.

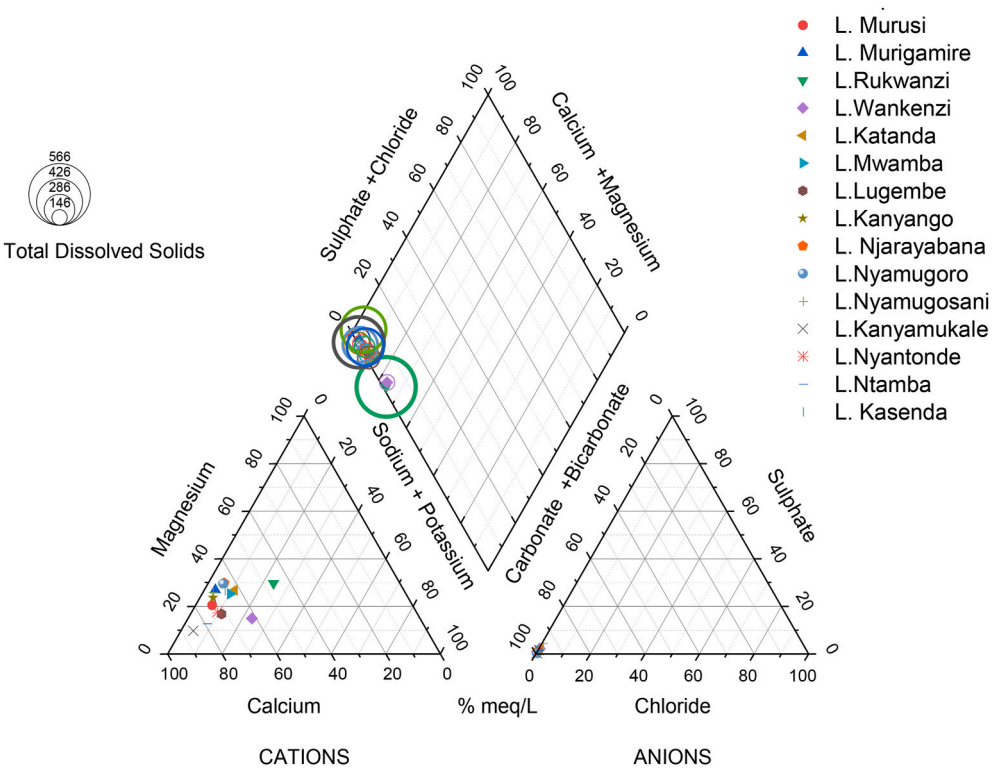

Fig. 2. Piper diagram for the Ndali-Kasenda crater lakes cluster.

3. Results and discussion

3.1. Ndali- Kasenda crater lakes water chemistry

A statistical summary of hydrochemical parameters of the analyzed crater lake water samples is presented in Table 1 and Table S1 (supplementary material). The pH values of the crater lake waters varied from 8.61 to 9.96 with a mean value of 9.37, reflecting the alkaline nature of groundwater in the Ndali-Kasenda crater lake cluster signaling dissolution of carbonates as bicarbonate. EC was in the range of 265–1180 μs/cm with an average of 551.15 ± 35.41 μs/cm with 6 % of sampled lakes exceeding the WHO (2017) limit of 1000 μs/cm while 33.33% exceeded the EC limits of USEPA (2012) standard of 500 μs/cm. The TDS ranged from 136 to 586 mg/L, indicating wide variation in the salt content of the lakes as a result of weathering and evaporation occurring to different extents due to vegetation cover (Khatri et al., 2020). Accordingly, TDS concentration is a basis for classifying water as fresh (<1000 mg/L); brackish (1000–10,000 mg/L); saline (10, 000–100,000 mg/L) and brine (>100,000 mg/L) (Ali et al., 2018; Bazaanah and Dakurah, 2021). Basing on this simple classification, all the lakes are alkaline and fresh since water samples from them had TDS below 1000 mg/L. All the values of TDS were below WHO (2017) and USEPA (2018) standards and strongly correlated with F^-, Cl^-, HCO_3^-, K^+, Ca^{2+}, $Mg^{2+}$and Mn^{2+}. The high EC and TDS in the Ndali- Kasenda lake waters may be attributed to sustained and widespread agriculture coupled with the natural geological conditions leading to the release of a high concentration of dissolved minerals into the lakes.

General dominance of the cations was in the order of $Ca^{2+} > Mg^{2+} > Na^+ > K^+ > Mn^{2+} > Al^{3+} >$ Fe while dominance of anions was in the order of $HCO_3^- > CO_3^{2-} > SO_4^{2-} > F^- > PO_4^{3-} > Cl^- > NO_3^-$. Ca^{2+} and Mg^{2+} concentrations were in the range 36–1540 mg/L with mean of 153.92 ± 25.94 mg/L and 13.44–119.5 mg/L with 45.33 ± 3.09 mg/L as mean value respectively. The total hardness (TH) varied from 136 to 448 mg/L with an average value of 286.22 ± 12.97 mg/L 13.33 % of the lakes had Ca^{2+} concentration above the maximum permissible WHO (2017) limit of 200 mg/L. Furthermore, 33.33 % had Mg^{2+} concentration above the desirable limit (50 mg/L) but were all below the maximum allowable limit of (150 mg/L) of the WHO (2017). Variation in Ca^{2+} and Mg^{2+} concentration corresponded to water hardness variation and can be explained by ion-exchange which removes Ca^{2+} and Mg^{2+} and replace them with Na^+ ions and dissolution of rocks in the lithosphere associated with the aquifers (Nyam et al., 2020). Na^+ and K^+ ranged from 4.25 to 32.00 mg/L with a mean of 12.12 ± 0.97 mg/L and 0.9–6.30 mg/L with a mean of 2.62 ± 0.19 mg/L respectively. Although Na^+ and K^+ were among the dominant cations, their concentrations were below the regulatory limits (WHO, 2017 and USEPA, 2018). The higher concentration of Ca^{2+}, Mg^{2+}, Na^+, and K^+ may be derived from weathering of felsic granites in the lithosphere in the Albertine graben and reverse cation exchange, accounting for water quality in the Ndali-Kasenda crater lakes (Arad and Morton, 1969; Guma et al., 2021). These findings are congruent with hydrogeochemical studies in the Albertine Graben groundwater quality that reported the alkaline carbonate-bicarbonate rich nature of the waters (Owor et al., 2021). The lower concentration of K^+ may be a result of its relative resistance to weathering of K-bearing minerals in potassic kamafugites and loss on soil surfaces while cation exchange and dissolution of evaporates and silicates occurring in the aquifer may also contribute to Na^+, accounting for its higher concentration in the lakes (de Dieu Ndikumana et al., 2020; Schneider et al., 2016). Al^{3+}, Mn^{2+}, and total iron were in the range 0.01–1.00 mg/L, 0.10–1.80 mg/L, and 0.004–21.820 mg/L respectively; attributed to weathering of minerals in rocks in the aquifers and erosion into the lakes. All studied lakes had high total iron content above WHO (2017) and US EPA (2018) arising from weathering of pyrite and magnetite minerals (de Dieu Ndikumana et al., 2020) while 80 % of lakes recorded manganese greater than permissible limits (WHO (2017) and USEPA (2018). Although iron is an important mineral for human health, its presence may not be hazardous but rather an aesthetic pollutant and a nuisance (Sarkar and Shekhar, 2018).

Among the anions HCO_3^- and CO_3^{2-} concentrations were highest ranging from 146 to 1307.84 mg/L with a mean of 582.64 ± 35.77 mg/L

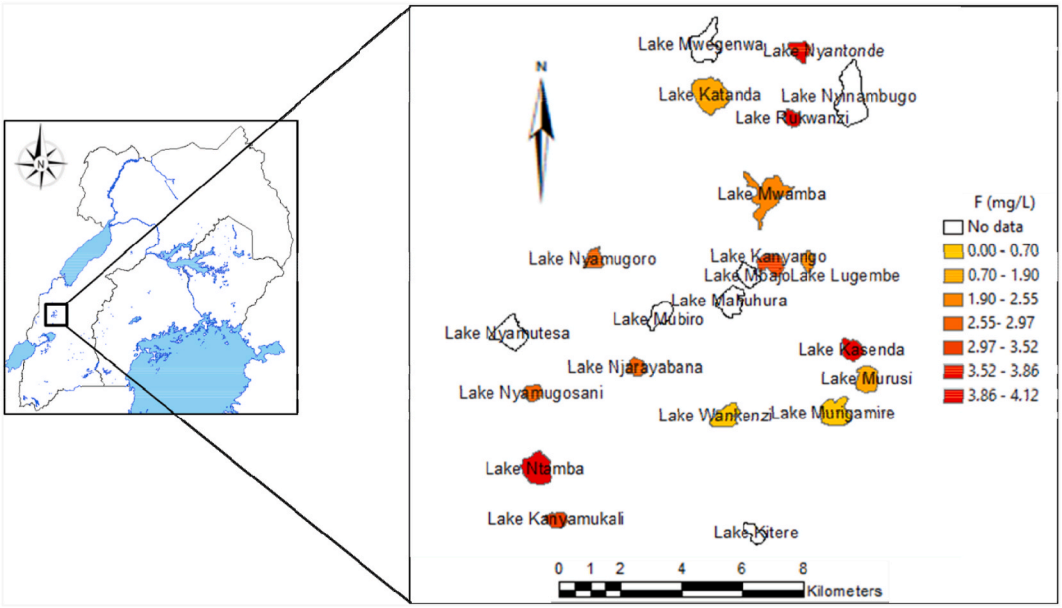

Fig. 3. Spatial variation of F^- concentration in the Ndali-Kasenda crater lakes cluster.

and 0–758.40 mg/L with a mean of 272.84 ± 19.71 mg/L respectively. The concentration of HCO_3^- in 53.33 % of studied crater lakes exceeded the WHO (2017) limit of 500 mg/L. The elevated levels of CO_3^{2-} and HCO_3^- in this area emanated from the natural dissolution of felsic granites, decay of organic matter in the unsaturated zone, volcanic carbon dioxide degassing, and permeation processes having interactions with the water table during recharge (Fenta et al., 2020; Guma et al., 2021; Kumarathilaka et al., 2016). In addition, SO_4^{2-} being another dominant anion in this area occurs commonly in groundwater with a high concentration (1000–1200 mg/L) causing a laxative effect on human systems (WHO, 2017). However, SO_4^{2-} concentration in the Ndali-Kasenda crater lakes attributed to oxidation of sulphides in the aquifer (Gawle et al., 2021) was in the range 1.0–47.24 mg/L, well below the standards. PO_4^{3-} ranged from 0.1 to 2.5 mg/L. This is attributable to weathering of phosphate minerals such as apatite found in the kamafugites, carbonatites, and francolite as well as erosion of phosphate-containing fertilizers from agricultural fields in the area (Nyam et al., 2020; Rosenthal et al., 2009; Tumwebaze et al., 2019). 93.33 % of the studied lakes had a mean PO_4^{3-} concentration above 0.3 mg/L prescribed as a maximum permissible limit in drinking water (WHO, 2017). NO_3^- ranged from 0.99 to 5.73 mg/L with an average of 2.12 mg/L, arising from leaching as water percolates into the water table as well as surface runoff carrying fertilizer, animal excreta, and agricultural by-products into the crater lakes (Kumarathilaka et al., 2016; Pathak and Bhandary, 2020). The presence of NO_3^- and PO_4^{3-} in the crater lakes explains the proliferation of algae in these water bodies (Sharmin et al., 2020). Excessive Cl^- amounts are known to accelerate corrosion of metals in the water distribution system, which is especially pronounced in highly alkaline waters. However, Cl^- concentrations in the Ndali-Kasenda lakes are reported as 0.17–10.0 mg/L with a mean value of 2.05 mg/L. All sampled lakes had lower Cl^- levels than the regulatory limit of 250 mg/L WHO (2017) and USEPA (2018). The presence of Cl^- in the lakes may be a result of weathering of rocks in the underlying geology of the lakes, leaching from the soils, domestic wastes, fertilizers, and surface runoff (us Saba et al., 2016).

BOD, COD and DO were in the range of 8.00–141.00 mg/L, 2.00–288.00 mg/L and 0.80–10.80 mg/L respectively. The BOD and COD may be attributed to the biochemical oxidation of organic matter and other oxidizable materials in the lakes (Mishra et al., 2019). All studied lakes had higher BOD and DO concentrations exceeding 6 mg/L and 4–6 mg/L respectively as permissible limits in drinking water (Kumarathilaka et al., 2016). DO reveal the changes occurring in the biological parameters in the lakes due to aerobic or anaerobic phenomenon. The DO was attributable to the photosynthetic activity of algae and water was found to be suitable for natural lake habitats since DO values are highly affected by turbulence, salinity, temperature, and altitude (Pazand et al., 2018).

3.2. Crater lake hydrochemical facies

The hydrogeochemical facies of the Ndali-Kasenda cluster of crater lakes was characterized using Piper Trilinear diagrams (Fig. 2). The facies anchors on the premise that regions with perceptible characteristics of different anions' and cations' concentrations plot within the diamond field. It was observed that in the cation plot field the majority of crater lakes water samples plotted towards the Ca^{2+} and Mg^{2+} corners, indicating the dominance of these cations in water samples in the area. This may be attributed to the dissolution of dolomite, limestone, gypsum, silicate rocks, and cation exchange in the aquifer (Fenta et al., 2020; Nyam et al., 2020; Pazand et al., 2018).

Nonetheless, Na^+ and K^+ also contributed to the overall classification but of low magnitude. Similarly, the samples plotted mainly in the HCO_3^- and CO_3^{2-} zones, showing their dominance in the anion field. This further indicates weathering processes occurring in the area involving felsic granites, gypsum, limestone, silicates, dolomite minerals, decay of organic matter in the unsaturated zone, and volcanic carbon dioxide degassing (Fenta et al., 2020; Getenet et al., 2020).

Hence, the Ndali-Kasenda lakes are generally of bicarbonate type with Ca–HCO_3 type predominating although mixed types: Ca–Mg–HCO3 and Na–K–HCO3 also occur in the area. This finding confirms that the hydrochemistry in the studied crater lakes is influenced by primary processes such as weathering of rocks in the aquifer (Khatri et al., 2020; Pazand et al., 2018; us Saba et al., 2016). The chemical signature obtained using Piper classification agrees with findings on the hydrogeochemical signature of the Albertine graben where carbonate and bicarbonate were reported to be high (Guma et al., 2021; Owor et al., 2021) with a negligible contribution of secondary processes owing to low SO_4^{2-}, Cl^- and NO_3^- obtained in this study. These studies reported the major ions are of juvenile and meteoric sources, suggestive of rock water interaction processes.

Although a majority of researchers used Piper classification for groundwater, the studied crater lakes do not have inlets/outlets aside

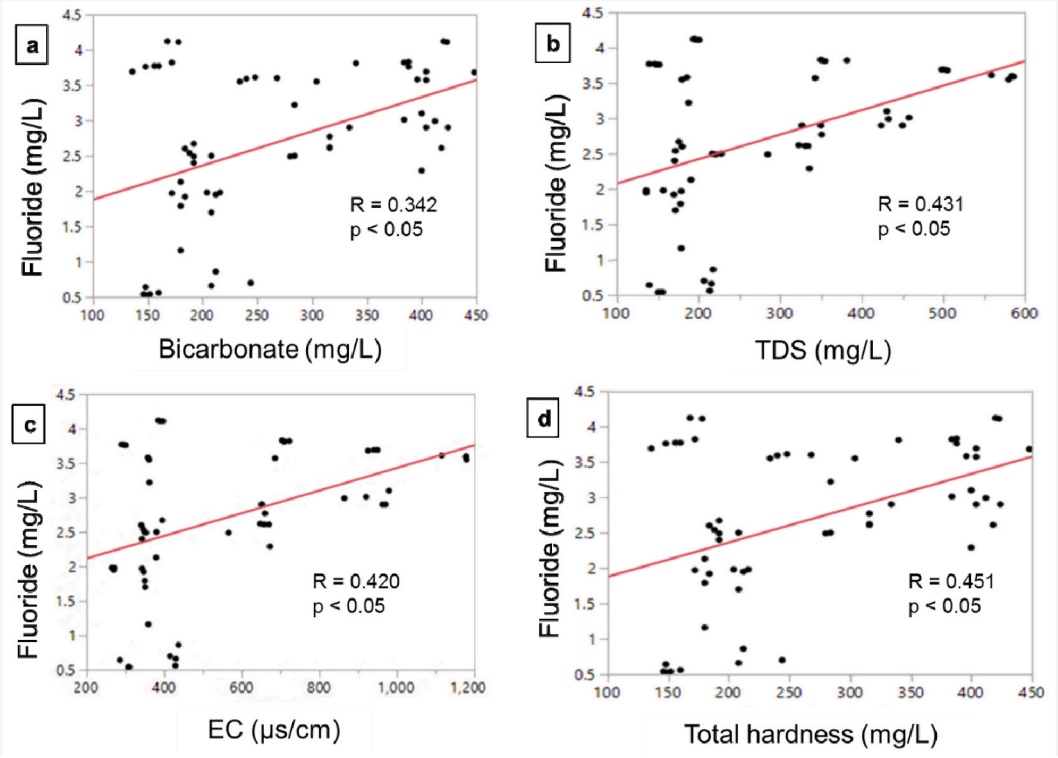

Fig. 4. Correlation plot between (a) F^- and bicarbonate, (b) F^- and TDS, (C) F^- and EC, (d) F^- and total hardness.

from L. Mwamba implying that they are groundwater-fed. Hence, their hydrogeochemistry may be taken to be similar to groundwater resources. The consequent interactions of crater lake waters with several rock types in the area induced an overall increase of TDS leading to a shift towards Na–K–HCO_3 with a parallel fluoride enrichment in the area.

3.3. *Fluoride geochemistry and spatial distribution*

In the present study, the concentration of F^- ranged from 0.53 to 4.12 mg/L with a mean of 2.69 ± 1.08 mg/L, indicating spatial variation in F^- concentration in the study area (Fig. 3). For instance, F^- concentration in 86.67 % of the crater lakes exceeded WHO (2017) while 73.33 % of the lakes had fluoride levels above USEPA (2018) regulatory limits. Accordingly, F^- concentration varied from 0.56 to 1.0 mg/L in 13.33% of the crater lakes, 1.1–2.0 mg/L in 13% of the lakes, 2.1–3.0 mg/L in 33.33% of the lakes and 3.1–4.1 mg/L in 40% of the crater lakes in the Ndali-Kasenda cluster (Fig. 3) (Fig. 4).

Based on the WHO (2017) standards, the Ndali- Kasenda lakes contain up to 2.75 times more F^- than the acceptable limit of 1.5 mg/L, much higher than that obtained in Sukulu hills (Eastern Uganda) in a study by Egor and Birungi (2020), in Kenya by Ontumbi et al. (2020) and Southwestern Nigeria by Emenike et al. (2018). However, the mean concentrations of F^- obtained in this study were comparable with those obtained in Rajasthan, India (Tiwari et al., 2020) but lower than those obtained from other studies from Kuhbanan basin in Central Iran (Pazand, 2016) rural Northwest China (Chen et al., 2017), Main Ethiopian Rift valley (Fenta et al., 2020) and Tanzania (Ijumulana et al., 2020). Since most of the lakes have no inlets or outlets (Fig. 1), their recharge water seems to come from underground aquifers and precipitation. The alkaline nature of the lake waters provided favorable conditions for fluoride enrichment by the dissolution of fluoride-containing rocks in the geology of the area (Ali et al., 2019; Guma et al., 2021; Mungoma, 1990; Bugenyi, Naluwairo, et al., 2015). High pH values encouraged the dissolution of carbonatite and fluoride minerals principally fluorspar (CaF_2) in the lake water since the excess –OH in the water disturbs the equilibrium for dissolution of CaF_2) as illustrated in chemical equations (5) and (6)

$$Ca(OH)_{2(aq)} \rightarrow Ca^{2+}(aq) + 2^{-}OH_{(aq)} \quad 5$$

$$CaF_{2(aq)} \longrightarrow Ca^{2+}{}_{(aq)} + 2F^{-}{}_{(aq)} \quad 6$$

Substitution of F^- by –OH ions or vice versa within the minerals by this mechanism is possible due to similarity in their ionic radii (Ali et al., 2019; Pazand, 2016). The release of fluoride into the water by this mechanism is controlled by the degree of saturation of fluorite and calcite as well as the amounts of Ca^{2+}, Na^+, and HCO_3^- in the water (Khatri et al., 2020). The saturation indices of aragonite, fluorite, calcite, anhydrite, gypsum, and dolomite that affect the fluoride release mechanism in water calculated using PHREEQC are in Table S4 and Fig. S5. From Fig. S5, aragonite and dolomite are both saturated implying that their precipitation is dominant to dissolution in the Ndali-Kasenda crater lakes while calcite, halite, fluorite, and gypsum are undersaturated that favors their dissolution to release F^-, halides, Mg^{2+} and Ca^{2+} into the water.

A positive correlation of F^- existed with pH ($r = 0.12$) signifying the contribution of high alkalinity in activating leaching of F^- into the crater lakes, though of low magnitude. Similarly, F^- dissolution from rock - water interaction accounted for by the moderate positive correlation with HCO_3^- ($r = 0.342$, $p < 0.05$) agrees with PHREEQC analysis, total hardness (TH) ($r = 0.451$, $p < 0.01$), TDS ($r = 0.431$, $p < 0.05$), chloride ($r = 0.29$, $p < 0.05$). Whereas other researchers found a positive and significant correlation of F^- with Ca^{2+} and Na^+ (Chen et al., 2017; Pazand, 2016), contrary results were obtained for this study while Mg^{2+} is marginally positive. This inconsistency may be due to the recharge and mixing of different recharge waters. Fluoride enrichment on account of high HCO_3^- concentration, EC, and TDS is in agreement with other findings (Emenike et al., 2018; Jha and Tripathi, 2021). This is because the high concentration of HCO_3^- in water suppresses the concentration of Ca^{2+} in the lakes thereby inducing F- enrichment (Jha and

Tripathi, 2021) according to equation (7):

$$CaF_{2(aq)} + 2HCO_3^{-}{}_{(aq)} \longrightarrow CaCO_{3(s)} + H_2O(l) + CO_{2\ (g)} + 2F^{-}{}_{(aq)} \quad 7$$

This is in agreement with earlier findings by other researchers in other water resources (Chen et al., 2017; Emenike et al., 2018).

In furtherance of this, the greater concentration of TDS enhanced the ionic strength and led to a rise in solubility of F^- containing minerals in the lakes. The rock-water interaction in the Ndali-Kasenda aquifers is key in the release of F^- into the lakes as reflected from Pearson's correlation coefficient (Table S2). In addition, the study area sits on a geothermal hot spot of the Albertine Rift valley which further facilitates fluoride dissolution (Bahati, 1993; Guma et al., 2021; Shah et al., 2021).

3.4. Multivariate statistical analysis

3.4.1. Cluster analysis

Cluster analysis (CA) is a widely used technique (Kumar et al., 2020; Nyam et al., 2020; Pazand et al., 2018) in water quality evaluation to decipher information on similarities/dissimilarities among sampling sites. In this study, spatial variability of hydrogeochemical variable in Ndali-Kasenda cluster was determined from CA using the complete linkage distance, reported as D_{link}/D_{max} which represents the quotient between the linkage distances for a particular case divided by the maximal Euclidean distance (Walter et al., 2019; Zhang et al., 2020). Based on the 23 hydrogeochemical variables, cluster analysis classified the 15 crater lakes into distinct clusters at D_{link}/D_{max}, reflecting the level of similarity in hydrogeochemistry among the lakes. Lakes: Murusi, Murigamire, and Kanyango are seen to be approximately 70% similar, Wankenzi, Kasenda, Mwamba, Nyantonde, and Lugembe with more than 70 % similarity while Rukwanzi, Njarayabana, Nyamugoro, Nyamugosani, Ntamba, and Kanyamukali are seen to be approximately 35 % similar.

The similarity in hydrogeochemistry in these lakes may be attributed to the Rift valley faulting in the basement leading to strongly metamorphosed and deformed amphibolites, quartzites, marbles, metasediments, and metavolcanic (Fenta et al., 2020). The weathering of volcaniclastic sediments containing bentonite, kaolin, gypsum, feldspar, pozzolana, appetite, francolite, vermiculite, zeolite deposits, and geomorphological intrusions of adamellite gneisses with post-orogenic alkaline biotite granites, sub-alkaline peraluminous equigranular aplitic and pegmatitic rocks with accumulated clastic gravels, silica sand, silts, limestone, gypsum, ball clays with Na, K, Mg salts (Andrade et al., 2020; Fenta et al., 2020) releases varying amounts of mineral ions in different lakes with varying physical and chemical environments leading to the observed dissimilarities in hydrogeochemical composition. Accordingly, the saturation indices calculated using PHREEQC indicated that the crater lake cluster: Murusi, Murigamire, and Kanyango are saturated concerning aragonite, dolomite, calcite, gibbsite, goethite, and hematite which makes precipitation of such minerals more likely than their dissolution (Fig. S2). In the cluster L. Wankenzi, L. Kasenda, L. Mwamba, L. Nyantonde, and L. Lugembe; vivianite, rhodochrosite, and hydroxylapatite are saturated in addition to minerals mentioned in the first cluster while in cluster comprising of Lakes: Rukwanzi, Njararyabana, Nyamugoro, Nyamugosani, Ntamba, and Kanyamukali, siderite is also saturated in addition to the minerals mentioned in the first two clusters. Even among the lakes in each cluster, there are notable differences in saturation indices, for example in L. Mwamba, calcite, aragonite, and dolomite are all soluble as predicted by PHREEQC (Fig. S2 and Table S4). The difference in relative saturation of the lakes with different minerals accounts for the observed dissimilarity among the lakes as observed in the spatial distribution of the hydrogeochemical data (Table S1).

3.4.2. Principal component analysis

Principal component analysis (PCA) is a broadly used technique that elucidates variation in a multivariate data set offering a means of identifying similarities among them and deciphering the structural activity relations thereby reducing the multidimensionality of the data (Fenta et al., 2020; Nyam et al., 2020; Ojok et al., 2017). It has been widely applied in water quality evaluation to obtain the ions controlling the hydrogeochemical processes by extracting factors associated with the hydrogeochemistry (Das et al., 2015; Emenike et al., 2018; Ojok et al., 2017). Correlation between the principal components and each of the hydrogeochemical variables is represented by the PC loadings. In water quality studies, principal components (PC) are usually interpreted in terms of geochemical processes such as rock-water interactions, by scrutiny of the loadings of original hydrogeochemical variables on each of the principal components (Egbueri, 2020; Laxmankumar et al., 2019; Nyam et al., 2020). The first PC contains the highest Eigenvalue, accounting for the highest variance of all the processes determining hydrogeochemistry in the lake. In this study, PCA was performed on 60 water samples from 15 crater lakes, reducing them into six PCs, cumulatively explaining 88.6 % of the data variance (Table 2 and Fig. S1) (supplementary material), although the first two PCs explained most of the variation in hydrochemical data obtained in this study.

Table 2
Principal components, loadings and percentage of variance explained.

Hydrochemical Variable	Principal components		
	PC1	PC2	PC3
Temp	−0.022	0.2	−0.242
EC	0.177	**0.361**	−0.06
pH	−0.035	**−0.335**	0.081
TDS	0.179	**0.363**	−0.045
Sulfate	0.067	0.067	−0.155
Fluoride	0.038	0.198	−0.073
Chloride	**0.322**	0.103	−0.132
Carbonate	**0.279**	−0.166	0.016
Carbonate	0.062	**0.344**	0.097
Nitrate	0.081	−0.05	**0.397**
Phosphate	0.222	−0.053	**0.417**
Sodium	**0.352**	−0.043	0.041
Potassium	**0.351**	−0.017	0.039
Calcium	−0.058	**0.332**	0.024
Magnesium	−0.009	**0.339**	0.201
Aluminium	0.002	0.047	**0.434**
Total Iron	−0.026	0.067	**0.529**
Manganese	**0.363**	−0.056	−0.032
Total hardness	−0.062	**0.353**	0.066
BOD	0.349	−0.086	0.01
COD	0.289	−0.095	−0.102
DO	−0.033	0.047	0.027
Eigen value	6.892	5.640	2.816
Percent of variance	**30**	**24.5**	**12.2**
Cumulative %	**30**	**54.5**	**66.7**

EC = electrical conductivity, BOD=Biological oxygen demand, COD= Chemical Oxygen demand, DO = dissolved oxygen, TDS = total dissolved solids, and Temp = temperature.

PC 1 had positive loadings of Cl^- (r = 0.322), CO_3^{2-} (r = 0.279), Na^+ (r = 0.352), K^+ (r = 0.351) and Mn^{2+} (r = 0.363), explaining 30% of the total variance and represents a combination of processes involving chemical weathering and mineralogical dissolution of rock constituents. Considering the loadings given above, PC1 may be regarded as a salinity factor. It is accounted for by dissolution of carbonate minerals such as dolomite, porphyritic biotite granite, porphyroblastic gneiss, ball clays with Na, K, Mg salts, limestone, silicates, and halites found in the geology of the area with evaporating deposits and the high rate of evaporation of water from the lakes that is typical in the tropics and semi-arid climates (Nyam et al., 2020; Shah et al., 2021; Tiwari et al., 2020) which accounted for the dominance of Na^+, Mn^{2+}, K^+, CO_3^{2-}, and Cl^- in the area. In addition, cations exchange processes involving sodium-montmorillonite could have contributed to Na^+ ion concentration as well.

PC 2 is dominated by positive loadings of EC (r = 0.361), TDS (r =

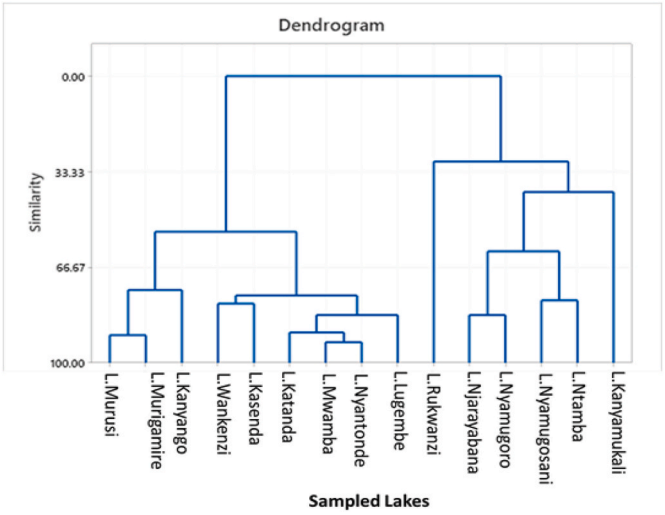

Fig. 5. Dendrogram for Ndali-Kasenda crater lakes based on hydrochemical characteristics.

0.363), Ca^{2+} (r = 0.332), Mg^{2+} (r = 0.339) HCO_3^- (r = 0.292), TH (r = 0.353) and negative loading of pH (r = −0.335), contributing 24.5 % of the total variance. This is depicted in the score plot of PC2 (24.5 %) against PC1 (30%) (Fig. S1). Looking at the loadings on this PC, it may be termed as an alkalinity index. This is suggestive of reactions involving silicate and carbonate minerals such as calcite, dolomite, porphyritic biotite granite, porphyroblastic gneiss, ball clays, and limestone, which are reported to occur in the area with evaporate deposits (Fenta et al., 2020; Shah et al., 2021). This could have resulted in the high alkalinity, total hardness and TDS observed during this study.

The dissolution of carbonate minerals like limestone, calcite, dolomite, and ball clays contributed to TDS, Ca, Mg, and HCO_3^- ions in the recharge zones of the lakes (PC2). The replacement of Na^+ ions by Ca^{2+} and Mg^{2+} ions from the hydrogeochemical matrix due to cation exchange processes with increasing residence time in the aquifer led to an increase in Na^+ ion concentration, as depicted in PC1(Kumar et al., 2020). Furthermore, sodic plagioclase field spars that occur in many geological settings tend to dissolve in carbonic acid-containing water and is one other process contributing to the observed Na^+ concentration in the groundwater-fed crater lakes (Fenta et al., 2020; Shah et al., 2021).

3.5. Human health risk due to fluoride exposure

Health risks associated with intake of water from Ndali-Kasenda lakes by infants (age 0–2 years), children (age 3–11 years), teenagers (age 12–19 years), and adults (age 20–65 years) using hazard quotient (HQ) were computed using parameters presented in Table S5. The non-carcinogenic risks were calculated for the studied crater lakes in the Ndali-Kasenda cluster and results are presented in Table S3 and Fig. 6. The average EDI values were in the range 0.0618–0.4522 mg/kg. day for infants, 0.0254–0.1721 mg/kg. day for children, 0.0038–0.0257 mg/kg. day for teens, and 0.0040–0.0267 mg/kg. day for adults (Table S3).

The health risks due to ingestion of crater lake water are as follows: 100% of the sampled lakes contained fluoride concentration that is likely to pose health risks to infants as the HQ values exceeded 1 (HQ > 1) while 86.67 % of lakes pose potential risks to children who ingest water from them (Fig. 5). However, the HQ for teens and adults was below 1, meaning water from the lakes does not pose any potential non-carcinogenic risks when ingested by teens and adults. HQ results obtained in this study are generally higher than those obtained in Southwestern Nigeria by Emenike et al. (2018) but are comparable with those obtained in Northwest China by Chen et al. (2017). From the HHRA model, it can be concluded that ingestion of water from the crater lakes could cause non-carcinogenic ill health in humans, especially infants and children. Hence there is a need for remediation to avert the negative health effects of excess fluoride in water from such lakes which are reported to be a health hazard causing dental fluorosis, skeletal fluorosis, neurological diseases (Ali et al., 2016; Edmunds and Smedley, 2005; Jha and Tripathi, 2021; Kashyap et al., 2020), carotid atherosclerosis (Jha and Tripathi, 2021), cardiac failure (Kimambo et al., 2019) and kidney disease (Ali et al., 2016; Edmunds and Smedley, 2005).

4. Conclusion

In this study, hydrochemical characteristics of 15 crater lakes in the Ndali-Kasenda cluster were studied for drinking purposes using hydrogeochemical, multivariate statistical techniques, and USEPA human health risks assessment method. Hydrochemical parameters show a wide range of variation as depicted in spatial fluoride Arc GIS map and cluster analysis with WHO (2017) regulatory limit exceedance observed on F^-, Ca^{2+}, pH, Fe, TDS, and Mn^{2+} for most of the studied lakes. From the piper diagram, it was observed that all the crater lakes were alkaline, with the main hydrogeochemical signature being Ca–HCO_3 (73.3%) and Ca–Mg–HCO_3 (20.0%) type. PCA performed on Ndali-Kasenda

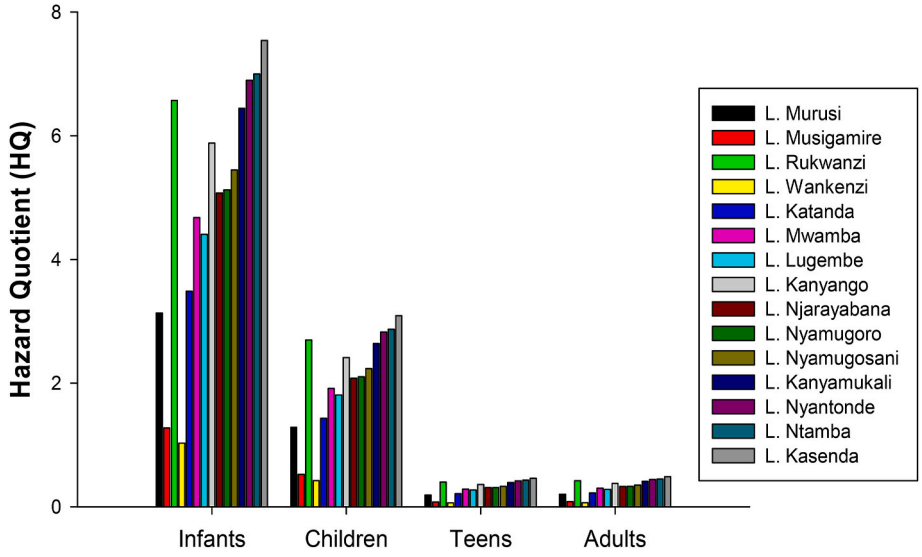

Fig. 6. Hazard quotient (HQ) for ingestion of Ndali- Kasenda crater lakes water.

hydrogeochemical data identified weathering of rocks reactions, ion exchange, and evaporation processes as the primary processes controlling the Ndali- Kasenda crater lake hydrogeochemistry. From the HHRA model, ingestion of water from all the studied lakes could pose potential non-carcinogenic morbidities in infants while 86.67% of the lakes may pose potential health risks to children. This showed that infants and children are more vulnerable to fluoride contamination in the crater lakes of Ndali-Kasenda than teens and adults.

Declaration of competing interest

The authors declare that they have no known competing financial interests or personal relationships which have or could be perceived to have influenced the work reported in this article.

Acknowledgments

The authors wish to acknowledge the financial assistance from the German Academic Exchange Service (DAAD) [Grant number: 91672385], Mbarara University of Science and Technology, and the technical assistance rendered by National Water and Sewerage Corporation, Mbarara Laboratory.

Appendix A. Supplementary data

Supplementary data to this article can be found online at https://doi.org/10.1016/j.gsd.2021.100650.

References

Ali, S., Fakhri, Y., Golbini, M., Thakur, S.K., Alinejad, A., Parseh, I., Shekhar, S., Bhattacharya, P., 2019. Concentration of fluoride in groundwater of India: a systematic review, meta-analysis and risk assessment. Groundwater for Sustainable Development 9, 100224.

Ali, S., Shekhar, S., Bhattacharya, P., Verma, G., Chandrasekhar, T., Chandrashekhar, A. K., 2018. Elevated fluoride in groundwater of Siwani Block, Western Haryana, India: a potential concern for sustainable water. Groundwater for Sustainable Development 7, 410–420.

Ali, S., Thakur, S.K., Sarkar, A., Shekhar, S., 2016. Worldwide contamination of water by fluoride. Environ. Chem. Lett. 14 (3), 291–315.

Andrade, C., Cruz, J.V., Viveiros, F., Coutinho, R., 2020. Diffuse CO2 emissions from Sete Cidades volcanic lake (São Miguel Island, Azores): influence of eutrophication processes. Environ. Pollut. 115624.

Apha, 2012. Standard Methods for the Examination of Water and Wastewater, vol. 10. American Public Health Association, Washington, DC.

Arad, A., Morton, W.H., 1969. Mineral springs and saline lakes of the western Rift valley, Uganda. Geochem. Cosmochim. Acta 33 (10), 1169–1181.

Bahati, G., 1993. Geochemical Studies on Waters from the Katwe-Kikorongo, Buranga and Kibiro Geothermal Areas. United Nations University, Uganda.

Bai, R., Huang, Y., Wang, F., Guo, J., 2020. Associations of fluoride exposure with sex steroid hormones among US children and adolescents, NHANES 2013–2016. Environ. Pollut. 260, 114003.

Bailey, K., Lloyd, F., Kearns, S., Stoppa, F., Eby, N., Woolley, A., 2005. Melilitite at Fort Portal, Uganda: another dimension to the carbonate volcanism. Lithos 85 (1–4), 15–25.

Bazaanah, P., Dakurah, M., 2021. Comparative analysis of the performance of rope-pumps and standardized handpumps water systems in rural communities of the northern and upper east regions of Ghana. Groundwater for Sustainable Development 13, 100563.

Bodrud-Doza, M., Islam, S.M.D.-U., Rume, T., Quraishi, S.B., Rahman, M.S., Bhuiyan, M. A.H., 2020. Groundwater quality and human health risk assessment for safe and sustainable water supply of Dhaka City dwellers in Bangladesh. Groundwater for Sustainable Development 10, 100374.

Chandrajith, R., Diyabalanage, S., Dissanayake, C.B., 2020. Geogenic fluoride and arsenic in groundwater of Sri Lanka and its implications to community health. Groundwater for Sustainable Development 10, 100359.

Chen, J., Wu, H., Qian, H., Gao, Y., 2017. Assessing nitrate and fluoride contaminants in drinking water and their health risk of rural residents living in a semiarid region of Northwest China. Exposure Health 9 (3), 183–195.

Das, N., Patel, A.K., Deka, G., Das, A., Sarma, K.P., Kumar, M., 2015. Geochemical controls and future perspective of arsenic mobilization for sustainable groundwater management: a study from Northeast India. Groundwater for Sustainable Development 1 (1–2), 92–104.

de Dieu Ndikumana, J., Bolarinwa, A.T., Adeyemi, G.O., Olajide-Kayode, J., Nambaje, C., 2020. Geochemistry of feldspar and muscovite from pegmatite of the Gatumba area, Karagwe Ankole Belt: implications for Nb–Ta–Sn mineralisation and associated alterations. SN Appl. Sci. 2 (9), 1–12.

Dongzagla, A., Jewitt, S., O'Hara, S., 2019. Assessment of fluoride concentrations in drinking water sources in the Jirapa and Kassena-Nankana Municipalities of Ghana. Groundwater for Sustainable Development 9, 100272.

Eby, G.N., Lloyd, F.E., Woolley, A.R., 2009. Geochemistry and petrogenesis of the Fort Portal, Uganda, extrusive carbonatite. Lithos 113 (3–4), 785–800.

Edmunds, W.M., Smedley, P.L., 2005. In: Alloway, B.J., Selinus, O. (Eds.), Fluoride in Natural Waters Essentials of Medical Geology. Elsevier, London.

Egbueri, J.C., 2020. Groundwater quality assessment using pollution index of groundwater (PIG), ecological risk index (ERI) and hierarchical cluster analysis (HCA): a case study. Groundwater for Sustainable Development 10, 100292.

Egor, M., Birungi, G., 2020. Fluoride contamination and its optimum upper limit in groundwater from Sukulu Hills, Tororo District, Uganda. Sci. African 7, e00241.

El Alfy, M., Abdalla, F., Moubark, K., Alharbi, T., 2019. Hydrochemical equilibrium and statistical approaches as effective tools for identifying groundwater evolution and pollution sources in arid areas. Geosci. J. 23 (2), 299–314.

Emenike, C.P., Tenebe, I.T., Jarvis, P., 2018. Fluoride contamination in groundwater sources in Southwestern Nigeria: assessment using multivariate statistical approach and human health risk. Ecotoxicol. Environ. Saf. 156, 391–402.

Fenta, M.C., Anteneh, Z.L., Szanyi, J., Walker, D., 2020. Hydrogeological framework of the volcanic aquifers and groundwater quality in Dangila Town and the surrounding area, Northwest Ethiopia. Groundwater for Sustainable Development 11, 100408.

Gawle, S., Pateria, K., Mishra, R.P., 2021. Physico-chemical analysis of groundwater during monsoon and winter season of Dindori district, India. Groundwater for Sustainable Development 12, 100550.

Getenet, M., García-Ruiz, J.M., Verdugo-Escamilla, C., Guerra-Tschuschke, I., 2020. Mineral vesicles and chemical gardens from carbonate-rich alkaline brines of lake magadi, Kenya. Crystals 10 (6), 467.

Guma, B.E., Muwanga, A., Owor, M., 2021. Hydrogeochemical evolution and contamination of groundwater in the Albertine Graben, Uganda. Environ. Earth Sci. 80 (8), 1–17.

Ijumulana, J., Ligate, F., Bhattacharya, P., Mtalo, F., Zhang, C., 2020. Spatial analysis and GIS mapping of regional hotspots and potential health risk of fluoride concentrations in groundwater of northern Tanzania. Sci. Total Environ. 139584.

Jha, P.K., Tripathi, P., 2021. Arsenic and fluoride contamination in groundwater: a review of global scenarios with special reference to India. Groundwater for Sustainable Development 100576.

John, R., Ezekiel, M., Philbert, C., Andrew, A., 2008. Schistosomiasis transmission at high altitude crater lakes in Western Uganda. BMC Infect. Dis. 8 (1), 1–6.

Kashyap, C.A., Ghosh, A., Singh, S., Ali, S., Singh, H.K., Chandrasekhar, T., Chandrasekharam, D., 2020. Distribution, genesis and geochemical modeling of fluoride in the water of tribal area of Bijapur district, Chhattisgarh, central India. Groundwater for Sustainable Development 11, 100403.

Khatri, N., Tyagi, S., Rawtani, D., Tharmavaram, M., Kamboj, R.D., 2020. Analysis and assessment of ground water quality in Satlasana Taluka, Mehsana district, Gujarat, India through application of water quality indices. Groundwater for Sustainable Development 10, 100321.

Kimambo, V., Bhattacharya, P., Mtalo, F., Mtamba, J., Ahmad, A., 2019. Fluoride occurrence in groundwater systems at global scale and status of defluoridation–state of the art. Groundwater for Sustainable Development 100223.

Kumar, P.J.S., Jegathambal, P., Babu, B., Kokkat, A., James, E.J., 2020. A hydrogeochemical appraisal and multivariate statistical analysis of seawater intrusion in point calimere wetland, lower Cauvery region, India. Groundwater for Sustainable Development 11, 100392.

Kumarathilaka, P., Jayawardhana, Y., Basnayake, B.F.A., Mowjood, M.I.M., Nagamori, M., Saito, T., Kawamoto, K., Vithanage, M., 2016. Characterizing volatile organic compounds in leachate from Gohagoda municipal solid waste dumpsite, Sri Lanka. Groundwater for Sustainable Development 2, 1–6.

Laxmankumar, D., Satyanarayana, E., Dhakate, R., Saxena, P.R., 2019. Hydrogeochemical characteristics with respect to fluoride contamination in groundwater of Maheshwarm mandal, RR district, Telangana state, India. Groundwater for Sustainable Development 8, 474–483.

Mendham, J., 2006. Vogels Textbook of Quantitative Chemical Analysis. Pearson Education India.

Mishra, S., Tiwary, D., Ohri, A., Agnihotri, A.K., 2019. Impact of municipal solid waste landfill leachate on groundwater quality in varanasi, India. Groundwater for Sustainable Development 9, 100230.

Mohanta, V.L., Singh, S., Mishra, B.K., 2020. Human health risk assessment of fluoride-rich groundwater using fuzzy-analytical process over the conventional technique. Groundwater for Sustainable Development 10, 100291.

Mungoma, S., 1990. The alkaline, saline lakes of Uganda: a review. Hydrobiologia 208 (1–2), 75–80.

Nankabirwa, A., De Crop, W., Van der Meeren, T., Cocquyt, C., Plisnier, P.-D., Balirwa, J., Verschuren, D., 2019. Phytoplankton communities in the crater lakes of western Uganda, and their indicator species in relation to lake trophic status. Ecol. Indicat. 107, 105563.

Nelson, P., 2003. Index to EPA Test Methods. United States Environmental Protection Agency, Region I.

Nyam, F.M.E.A., Yomba, A.E., Tchikangoua, A.N., Bounoung, C.P., Nouayou, R., 2020. Assessment and characterization of groundwater quality under domestic distribution using hydrochemical and multivariate statistical methods in Bafia, Cameroon. Groundwater for Sustainable Development 10, 100347.

Ojok, W., Wasswa, J., Ntambi, E., 2017. Assessment of seasonal variation in water quality in River Rwizi using multivariate statistical techniques, Mbarara Municipality, Uganda. J. Water Resour. Prot 9 (1), 83–97.

Onipe, T., Edokpayi, J.N., Odiyo, J.O., 2020. Review on the potential sources and health implications of fluoride in groundwater of sub-saharan Africa. J. Environ. Sci. Heal. Part A 2020, 1–16.
Ontumbi, G.M., Ucakuwun, E.K., Munyao, T.M., 2020. Variation of fluoride levels in surface geology: a study of river njoro catchment, Kenya. African J. Education Sci. Technol. 6 (1), 1–8.
Owor, M., Muwanga, A., Tindimugaya, C., Taylor, R.G., 2021. Hydrogeochemical processes in groundwater in Uganda: a national-scale analysis. J. Afr. Earth Sci. 175, 104113.
Pathak, D.R., Bhandary, N.P., 2020. Evaluation of groundwater vulnerability to nitrate in shallow aquifer using multi-layer fuzzy inference system within GIS environment. Groundwater for Sustainable Development 11, 100470.
Pazand, K., 2016. Geochemistry and multivariate statistical analysis for fluoride occurrence in groundwater in the Kuhbanan basin, Central Iran. Model. Earth Sys. Environ. 2 (2), 72.
Pazand, K., Khosravi, D., Ghaderi, M.R., Rezvanianzadeh, M.R., 2018. Identification of the hydrogeochemical processes and assessment of groundwater in a semi-arid region using major ion chemistry: a case study of Ardestan basin in Central Iran. Groundwater for Sustainable Development 6, 245–254.
Rosenthal, A., Foley, S.F., Pearson, D.G., Nowell, G.M., Tappe, S., 2009. Petrogenesis of strongly alkaline primitive volcanic rocks at the propagating tip of the western branch of the East African Rift. Earth Planet Sci. Lett. 284 (1–2), 236–248.
Rubaihayo, J., Moghusu, E., Clouds, P., Abaasa, A., 2008. Schistosomiasis at high altitude crater lakes in Western Uganda. BMC Infect. Dis. 8 (110), 6–11. https://doi.org/10.1186/1471-2334-8-110.
Sarkar, A., Shekhar, S., 2018. Iron contamination in the waters of Upper Yamuna basin. Groundwater for Sustainable Development 7, 421–429.
Saulnier-Talbot, É., Chapman, L.J., Efitre, J., Simpson, K.G., Gregory-Eaves, I., 2018. Long-term hydrologic fluctuations and dynamics of primary producers in a tropical crater lake. Frontiers Ecol. Evol. 6, 223.
Schneider, S., Hornung, J., Hinderer, M., Garzanti, E., 2016. Petrography and geochemistry of modern river sediments in an equatorial environment (Rwenzori Mountains and Albertine rift, Uganda)—implications for weathering and provenance. Sediment. Geol. 336, 106–119.
Shah, M., Pawar, Y., Patel, M., Patel, J., Patel, N., 2021. Comprehensive hydro-chemistry and geothermal water quality of Konkan, Maharashtra, India for sustainable industrial development. Groundwater for Sustainable Development 12, 100518.
Sharmin, A., Hai, M.A., Hossain, M.M., Rahman, M.M., Billah, M.B., Islam, S., Jakariya, M., Smith, G.C., 2020. Reducing excess phosphorus in agricultural runoff with low-cost, locally available materials to prevent toxic eutrophication in hoar areas of Bangladesh. Groundwater for Sustainable Development 10, 100348.
Singh, S.K., Srivastava, P.K., Gupta, M., Mukherjee, S., 2012. Modeling mineral phase change chemistry of groundwater in a rural-urban fringe. Water Sci. Technol. 66 (7), 1502–1510.
Singh, S.K., Srivastava, P.K., Pandey, A.C., 2013. Fluoride contamination mapping of groundwater in Northern India integrated with geochemical indicators and GIS. Water Sci. Technol. Water Supply 13 (6), 1513–1523.
Smedley, P.L., Nkotagu, H., Pelig-Ba, K., MacDonald, A.M., Tyler-Whittle, R., Whitehead, E.J., Kinniburgh, D., 2002. Fluoride in Groundwater from High-Fluoride Areas of Ghana and Tanzania.
Thakur, J.K., Singh, P., Singh, S.K., Bhaghel, B., 2013. Geochemical modelling of fluoride concentration in hard rock terrain of Madhya Pradesh, India. Acta Geologica Sinica-English Edition 87 (5), 1421–1433.
Tiwari, K.K., Krishan, G., Prasad, G., Mondal, N.C., Bhardwaj, V., 2020. Evaluation of fluoride contamination in groundwater in a semi-arid region, Dausa District, Rajasthan, India. Groundwater for Sustainable Development 11, 100465.
Toolabi, A., Bonyadi, Z., Paydar, M., Najafpoor, A.A., Ramavandi, B., 2021. Spatial distribution, occurrence, and health risk assessment of nitrate, fluoride, and arsenic in Bam groundwater resource, Iran. Groundwater for Sustainable Development 12, 100543.
Tumwebaze, I., Clewing, C., Dusabe, M.C., Tumusiime, J., Kagoro-Rugunda, G., Hammoud, C., Albrecht, C., 2019. Molecular identification of Bulinus spp. intermediate host snails of Schistosoma spp. in crater lakes of western Uganda with implications for the transmission of the Schistosoma haematobium group parasites. Parasites Vectors 12 (1), 1–23.
Ubos, 2019. Uganda bureau of statistics 2019 statistical abstract.
US EPA, 1989. Risk Assessment Guidance for Superfund. Human Health Evaluation Manual Part A, Part A (EPA/540/1-89/002). https://doi.org/EPA/540/1-89/002.
US EPA, 2011. Exposure Factors Handbook: 2011 Edition. U.S Environmental Protection Agency, 2011 Editi. https://doi.org/EPA/600/R-090/052F.
us Saba, N., Umar, R., Ahmed, S., 2016. Assessment of groundwater quality of major industrial city of Central Ganga plain, Western Uttar Pradesh, India through mass transport modeling using chloride as contaminant. Groundwater for Sustainable Development 2, 154–168.
Van Daele, J., Hulsbosch, N., Dewaele, S., Muchez, P., 2020. Metamorphic and metasomatic evolution of the western domain of the karagwe-ankole belt (central Africa). J. Afr. Earth Sci. 103783.
Walter, O., Wasswa, J., Nakiguli, C.K., Ntambi, E., 2019. Spatial variation in physicochemical surface water quality in river rwizi, western Uganda. J. Water Resour. Protect. 11 (12), 1427–1440.
Wanke, H., Ueland, J.S., Hipondoka, M.H.T., 2017. Spatial analysis of fluoride concentrations in drinking water and population at risk in Namibia. WaterSA 43 (3), 413–422.
WHO, 2017. *Guidelines For Drinking-Water Quality* (Fourth Edi). World Health Organization.
Zhang, Q., Xu, P., Qian, H., Yang, F., 2020. Hydrogeochemistry and fluoride contamination in Jiaokou Irrigation District, Central China: assessment based on multivariate statistical approach and human health risk. Sci. Total Environ. 741, 140460.